ISSN 2176-5480

22nd International Congress of Mechanical Engineering (COBEM 2013)
November 3-7, 2013, Ribeirão Preto, SP, Brazil

A REDUCED ORDER MODEL OF TWO AND THREE-DIMENSIONAL SLACK CABLES

Mario Raúl Escalante
FRCU, Universidad Tecnológica Nacional, C. del Uruguay (ER), Argentina and FRCon, Universidad Tecnológica Nacional, Concordia (ER), Argentina
escalam@frcu.utn.edu.ar

Marta Beatriz Rosales
Department of Engineering, Universidad Nacional del Sur, Bahía Blanca, Argentina and CONICET, Argentina
mrosales@criba.edu.ar

Rubens Sampaio
Department of Mechanical Engineering, Pontifícia Universidade Católica do Rio de Janeiro, Brazil
rsampaio@puc-rio.br

Thiago Ritto
Department of Mechanical Engineering, Universidade Federal do Rio de Janeiro, Brazil
tritto@mecanica.ufrj.br

Abstract. *Cables and other flexible pipes are found in many applications of Civil, Aerospace, and Mechanical Engineering. Many offshore problems involve slender rods or cables (pipelines, risers and mooring lines). To design efficient structures, usually non-linear unidimensional theories are used to predict their dynamic response. Here, two models are analyzed, two-dimensional and three-dimensional representations of a slack cable, respectively. Since an economical and efficient model is desired to perform parametric studies, a Proper Orthogonal Decomposition (POD) and a Galerkin projection are performed to obtain a Reduced Order Model (ROM) for each case. The plane cable case ROM is constructed using a basis derived from the dynamics of an inextensible chain (a similar and simpler problem). The three-dimensional cable is modeled considering also the bending and torsional rigidities. A POD is performed on an accurate dynamic model previously solved by a finite element discretization. Different dynamic actions are evaluated in both cases and verifications with complete models are shown. The response of the cables to prescribed, low and high speed, dynamic displacements at one of the ends is evaluated and in the tridimensional case, an end angular motion is added. The necessary number of Proper Orthogonal Modes is assessed.*

Keywords: *Dynamics of Cables, Proper Orthogonal Decomposition, Model Reduction.*

1. INTRODUCTION

Slack cables and chains are used, for instance, in mooring devices as well as in many structural applications, constituting dynamic systems that undergo nonlinear motions. The main source of the nonlinearity is inherently geometric Esmailzadeh and Goodarzi (2001); Rosales and Filipich (2006). Several researchers have published in this subject (Huang (1994); Liu and Bergdahl (1997); Pascoal *et al.* (2005); Esmailzadeh and Goodarzi (2001); Rosales and Filipich (2006)). Low-dimensional approximations for the full high-dimensional dynamical system, which retain the main features, are desirable. The Model Order Reduction (MOR) approach seeks to reduce the computational complexity and time of computation of large scale dynamical systems by stating approximations of much lower dimensions that can produce nearly the same input/output characteristics. A good approximation with a low dimensional model can be obtained by a Galerkin approach with a proper basis and thus a Reduced Order Model (ROM) is obtained. The availability of a ROM is very useful, for instance, to perform an uncertainty quantification. In effect, the stochastic modeling requires of an economical model from the computational point of view.

In this work, we use Proper Orthogonal Decomposition (POD), which has been widely discussed in the literature during the last decades. The technique provides an efficient way of capturing the dominant components of a multidimensional system and representing it to the desired precision by using the relevant set of modes, thus reducing the order of the system. The method is also known as Karhunen-Loève decomposition (Karhunen, 1946; Loève, 1946) or principal component analysis (Hoetelling, 1935). Further names are factor analysis or total least-squares estimation depending on the applications and certain conditions. It provides an optimally ordered, orthonormal basis in the least-squares sense for a given set of theoretical, experimental or computational data. Reduced order models or surrogate models are then obtained by truncating this optimal basis. The method of snapshots introduced by Sirovich (Sirovich, 1987) is one of the most relevant ones. Here, the data set is chosen as time snapshots containing the spatial distribution of a numerical simulation

ISSN 2176-5480

at certain time instances reflecting the system dynamics. As an *a posteriori* data dependent method, it does not need *a priori* knowledge of the system behaviour and can also be used to analyze patterns in data. In combination with Galerkin projection, it provides a powerful tool to derive surrogate models for high-dimensional or even infinite dimensional dynamical systems, since the subspace is composed of basis functions inheriting already special characteristics of the overall solution. This is in contrast to standard finite element discretizations where the choice of the basis functions is in general unrelated with the system dynamics. The main advantage of POD lies in the fact that it requires only standard matrix computations, despite of its application to nonlinear problems. Although projecting only onto linear or affine subspaces, the overall nonlinear dynamics is preserved since the surrogate model will still be nonlinear.

In this article, two cable models will be analyzed: a two-dimensional (2D) representation of a simple cable (neither bending nor torsional stiffness) and a three-dimensional (3D) cable taking into account the bending and torsional stiffness. In both cases, a MOR is applied. The dynamic response of slack cables subjected to self-weight and prescribed displacements movements at their ends is analyzed. The governing nonlinear system of partial differential equations, is then solved using Galerkin method. In the 2D, the POD is used to find a set of orthogonal functions (basis) from the study of the dynamical behavior of a chain with rigid links, which represents a simpler problem. They are after used to solve the governing equations of slack cables with the Galerkin method, and to find the ROM for the dynamic problem of slack cables. The use of this advantageous technique allows to solve a complex problem starting from a simpler one with similar characteristics. The dynamic behavior of a chain with rigid links is governed by a system of nonlinear ordinary system of differential algebraic equations (DAE) and was previously solved by the authors Filipich and Rosales (2007) by implementing power series algorithms, whereas the slack cables dynamics is governed by a system of partial differential equations. Finally, the chain dynamic response is employed to find the basis (POMs) which are then introduced in a Galerkin approximation of the PDE of the slack 2D cable.

The second model deals with a three-dimension representation of the cable accounting for bending and torsion. A twisted cubic spline element and a lumped mass approximation are stated to provide a representation of both the bending and torsional effects. Among the most advanced finite element methods proposed for nonlinear beams, the geometrically exact approach initiated by Simo (Simo, 1985) is probably one of the most efficient. In fact, the dynamic modelling of marine cables has been studied extensively since the early 1960's for the analysis of mooring line tensions (Walton and Polacheck, 1960). However, the topic of low-tension cable dynamics is of more recent interest. Grosenbaugh et al. (Grosenbaugh *et al.*, 1993) simulated the low tension tether motion of an underwater remotely operated vehicle (ROV) in two dimension using a finite difference approximation to the cable equations of motion and a representation of the tether bending stiffness. An alternative to the finite difference approach is the lumped mass strategy. In (Buckham and Nahon, 2001) the authors present and validate through experimentation, a lumped mass formulation for low tension cables that appends a bending stiffness model to a previously developed standard lumped mass formulation (Buckham *et al.*, 2003; Driscoll *et al.*, 2000). There are two drawbacks to the existing low-tension lumped mass formulation: it needs small linear elements to capture curvature variation, and there is currently no means for capturing the effects of a non-zero torsional stiffness. A cubic element type is introduced by (Buckham *et al.*, 2004) and the equations of motion for the continuous cable are discretized using this higher order element. The latter work develops a finite element cable model based on a third-order element with a reduced-order state vector. Following the developments of Garret (Garret, 1982) and Nordgren (Nordgren, 1974, 1982), the nonlinear equations of motion for the continuous tether in terms of an inertial frame of refererence using the Frenet equations, are developed. Finally, it will be shown that our particular choice of the finite element allows the assembled system of equations to be reduced into a system that has the same dimension as the simpler linear lumped parameter model, but yet mantains an accurate and complex representation of the higher order bending and torsional effects.

In both cases, numerical illustrations show the derivation of the ROMs and the most adequate number of PODs for each case.

2. PROPER ORTHOGONAL DECOMPOSITION (POD)

POD is a method for constructing a low-dimensional approximation representation of a subspace in a Hilbert space. It is essentially the same as the Singular Value Decompostion (SVD) in a finite-dimensional space or in Euclidean space. It efficiently extracts the basis elements that contain characteristics of the space of expected solutions of the PDE. The POD basis in Euclidean space may be specified formally as follows. Let $\{\mathbf{y}_1, \ldots, \mathbf{y}_m\}\,\mathbb{R}^n$ be a set of centered (with respect to the mean) snapshots (recall that snapshots are samples of trajectories) $\mathbf{y}_i = \mathbf{R}_i - \overline{\mathbf{R}}$ where $\mathbf{y}_i$ is the i-th centered snapshot, $\mathbf{R}_i$ is the i-th snapshot obtained from physical tests or numerical simulations and $\overline{\mathbf{R}}$ is the mean trajectory. Let $\mathcal{Y} = span\,\{\mathbf{y}_1, \ldots, \mathbf{y}_m\}\,\mathbb{R}^n$ and r is the rank of $\mathcal{Y}$. A POD basis of dimension $k < r$ is a set of orthonormal vectors $\{\phi\}_{i=1}^{k} \subset \mathbb{R}^n$ whose linear span best approximates the space $\mathcal{Y}$. The basis set $\{\phi\}_{i=1}^{k}$ solves the minimization problem

$$\min_{\{\phi\}_{i=1}^{k}} \sum_{j=1}^{m} \left|\left| \mathbf{y}_j - \sum_{i=1}^{k} (\mathbf{y}_j^T \phi_i)\phi_i \right|\right|_2^2 \quad \text{with} \quad \phi_i^T \phi_j = \delta_{ij} = \begin{cases} 1 & \text{if} \quad i = 1\,, \\ 0 & \text{if} \quad i \neq j, \end{cases} \qquad i, j = 1, \ldots, k. \tag{1}$$

ISSN 2176-5480

It is well known that the solution to Eq. (1) is provided by the set of the left singular vectors of the *snapshots matrix* $\mathbf{Y} = [\mathbf{y}_1, \ldots, \mathbf{y}_m]\mathbb{R}^{n\times m}$. In particular, suppose that the SVD of $\mathbf{Y}$ is

$$\mathbf{Y} = \mathbf{V}\mathbf{\Sigma}\mathbf{W}^T, \tag{2}$$

where $\mathbf{V} = [\mathbf{v}_1, \ldots, \mathbf{v}_n] \in \mathbb{R}^{n\times n}$ and $\mathbf{W} = [\mathbf{w}_1, \ldots, \mathbf{w}_m] \in \mathbb{R}^{m\times m}$ are orthogonal and $\Sigma \in \mathbb{R}^{n\times m}$ contains the singular values on its diagonal $(\sigma_1, \ldots, \sigma_r)$ with $\sigma_1 \geq \sigma_2 \geq \ldots \geq \sigma_r > 0$. The rank of $\mathbf{Y}$ is $r \leq \min(n, m)$. Then the POD basis or the optimal solution of Eq.(1) is $\{\mathbf{v}_i\}_{i=1}^k$. The minimum 2-norm error from approximating the snapshots using the POD basis is then given by

$$\sum_{j=1}^{m} \left|\left| \mathbf{y}_j - \sum_{i=1}^{k} (\mathbf{y}_j^T \phi_i)\phi_i \right|\right|_2^2 = \sum_{i=k+1}^{r} \sigma_i^2. \tag{3}$$

The choice of the snapshot ensemble is a crucial factor in constructing a POD basis. This choice can greatly affect the approximation of the original solution space, but is a separate issue and will not be discussed here. POD is a popular approach because it works well in many applications and often provides an excellent reduced basis. However, as discussed in the introduction, when POD is used in conjunction with the Galerkin projection, effective dimension reduction is usually limited to the linear terms or low-order polynomial nonlinearities. Systems with general nonlinearities need additional treatment (Chaturantabut and Sorensen, 2010). We refer the reader to (Kunisch and Volkwein, 2008) for more details on the POD basis in general Hilbert space.

3. TWO-DIMENSIONAL CABLE

3.1 Chain dynamics

In order to construct a low-order dynamical model to simulate the dynamical behavior of slack cables we analyze a simpler problem with similar characteristics, like a chain with rigid links. A POD is performed to obtain a basis which, afterwards is introduced in a Galerkin approximation to solve the cable dynamics problem. This approach has advantages and limitations. Within the first, we could mention the simplicity of the reference problem (dynamics of inextensible chains governed by ODE's) and with respect to the second, the dynamics of the cables should resemble that of the chain, e.g. a low frequency motion of a cable approximates a chain motion. For the sake of brevity, the chain dynamics problem is not stated and derived herein in detail and the reader is refered to Filipich and Rosales (2007); Escalante *et al.*. Only a short description is included to show the type of problem solved in order to obtain the POD bases that will be used later on in the construction of the ROM of the plane cable.

Figure 1a shows a scheme of a chain made of N inextensible links each of length a and uniform cross section, *i.e.* the chain total length is $L = Na$. There are $(N + 1)$ hinged nodes and N links. In general, the chain will be subjected, besides its self-weight, to arbitrary conservative and deterministic forces. The motion will give place to inertial forces and reactions at each node. As mentioned before, the focus will be on the dynamic problem with prescribed end displacements, *i.e.* $x_1(t)$, $y_1(t)$, $x_{N+1}(t)$ and $y_{N+1}(t)$ are input. A free body diagram of a generic portion k (a link) is sketched in Figure 1b. Coordinates and both, active and reaction forces and their directions, are depicted. The orthogonal cartesian axes XY are adopted as the inertial reference and geometric continuity is accepted at coincident nodes of consecutive links. At the same time, the forces H_1, V_1, H_{N+1} and V_{N+1} will arise from the prescribed displacements. The length element of the link $ds = dX$ is constant in time since the inextensibility assumption holds. If we denote ρ as the uniform density for all links, the mass element dm is $dm = \rho\Omega ds = \rho\Omega dX$, $\gamma = \rho g$ is the unit weight and g is the gravity acceleration. The active forces per unit length, variable in general with the link length, have the cartesian components p_k^* and q_k.

The governing equations of the inextensible chain are stated together with the inextensibility condition for each link. Also the initial conditions are given at the initial time. Thus, a system of $4N$ equations with $4N$ unknowns (x_k, y_k $(k = 2, 3, , N)$ and H_k, V_k $(k = 1, 2, , N + 1)$) is obtained (see Escalante *et al.*). This system is solved by a power series approach by representing the unknown time functions as follows $(k = 1, 2, \cdots, N + 1)(p = 1, 2, \cdots, N_p)$:

$$x_{pk}(\tau) = \sum_{j=0}^{\infty} A_{pkj}\tau^j \qquad y_{pk}(\tau) = \sum_{j=0}^{\infty} B_{pkj}\tau^j; \quad H_{pk}(\tau) = \sum_{j=0}^{\infty} C_{pkj}\tau^j \qquad V_{pk}(\tau) = \sum_{j=0}^{\infty} D_{pkj}\tau^j \tag{4}$$

3.2 Dynamics of slack extensible cables

Now, the dynamics of an extensible cable will be stated. Recall that the POD is performed using the chain dynamics (see Escalante *et al.*) and after that, the POMs are introduced in a Galerkin approximation to find the cable response. Figure 2a shows a free body diagram of a portion of a cable, in which the forces acting are detailed. Assuming that the

ISSN 2176-5480

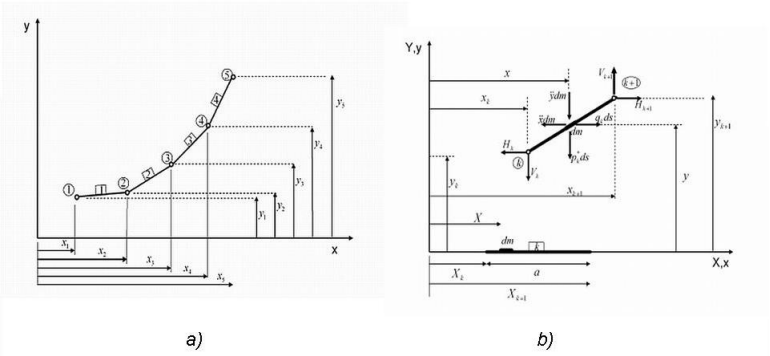

Figure 1: Rigid link chain. a) Four links chain. Coordinates of hinged nodes; b) Free body diagram of a link.

cable is extensible, the equations of motion of the cable are:

$$H' = \rho\Omega\Upsilon\ddot{x}, \qquad V' = \rho\Omega\Upsilon(\ddot{y} + g) \tag{5}$$

where the prime denotes derivative w.r.t. the spacial variable X, the dot w.r.t. time, $\Upsilon = ds/dX$ is the stretching and H and V are the horizontal and vertical components, respectively, of the static cable tension T, ρ is the cable density material, Ω is the cross section and g is the gravity acceleration.

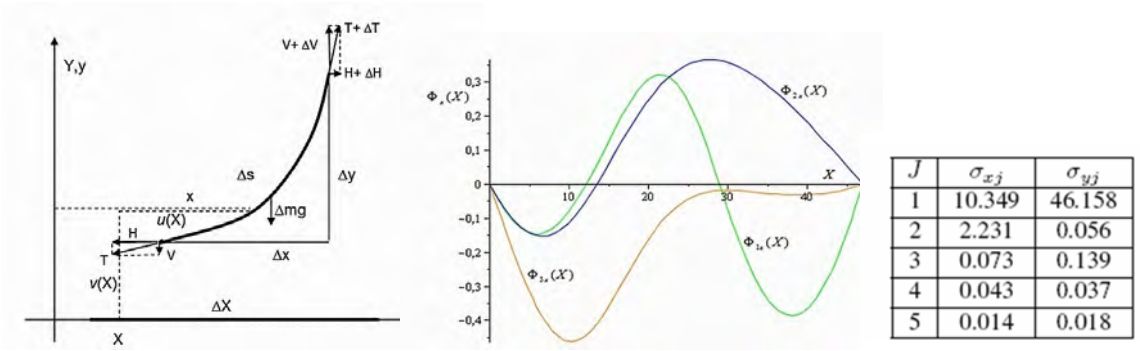

J	σ_{xj}	σ_{yj}
1	10.349	46.158
2	2.231	0.056
3	0.073	0.139
4	0.043	0.037
5	0.014	0.018

(a) (b) (c)

Figure 2: Plane cable. a) Slack cable portion. b) Three first Proper Orthogonal Modes (POMs) for the x displacement. c) First five singular orthogonal values.

Let us now propose a constitutive law for the cable material $T/\Upsilon = K(\Upsilon^2 - 1)/2$ which was discussed in Filipich and Rosales (2000). Then the governing equations are written as (K is a constant with axil stiffness units):

$$\left[x'\left(\Upsilon^2 - 1\right)\right]' = \frac{2\rho_0\Omega}{K}\ddot{x}; \quad \left[y'\left(\Upsilon^2 - 1\right)\right]' = \frac{2\rho_0\Omega}{K}(\ddot{y} + g) \tag{6}$$

4. Numerical examples

A cable of length $L = 47$ m with the left end fixed and the right one subjected to a prescribed motion given by the functions $x(L,t) = A + q_0\cos(\omega_q t)$ e $y(L,t) = B + h_0\cos(\omega_h t)$ is considered. The following data are adopted: $A = 37$ m, $B = 18$ m, $q_0 = 3$ m, $h_0 = 2$ m, $\omega_q = \omega_h = 0.25$ rad/s, and $2\rho_0\Omega/K = 1.8 \times 10^{-7}$/m. At first, the cable is in the static equilibrium position. To find the POMs, a similar problem of a chain with N rigid links was analyzed. The data matrices $\hat{X}$ and $\hat{Y}$ correspond to the geometric configuration of the chain (instantaneous horizontal and vertical coordinates at each node) at 51 time instants spaced 0.5 seconds. In order to obtain eigenmodes with higher energy contribution (*i.e.* $\epsilon = \sigma_i / \sum \sigma_i$) we need to construct the covariance matrix of the velocity vector field correlating all points in the domain. Then the average values are substracted as previously mentioned. The POD is then performed. Recall that the governing equations for the problem of the extensible cable are given by Eqs. 6 together with $x(0,t) = y(0,t) = 0, x(L,t) = F_1(t), y(L,t) = F_2(t)$. The following change of variables is introduced:

$$\hat{x} = x(X,t) - \frac{X}{L}F_1(t); \quad \hat{y} = y(X,t) - \frac{X}{L}F_2(t) \tag{7}$$

ISSN 2176-5480

The boundary conditions (BC) are $\hat{x}(0,t) = \hat{y}(0,t) = 0$ and $\hat{x}(L,t) = \hat{y}(L,t) = 0$. With this change of variables the basis of functions fulfill the BC at every instant. The POMs $\left\{\hat{\phi}_{1x}(X), ..., \hat{\phi}_{mx}(X)\right\}$ and $\left\{\hat{\phi}_{1y}(X), ..., \hat{\phi}_{my}(X)\right\}$ obtained from matrices $\tilde{X}_m$ and $\tilde{Y}_m$, are already expressed in the new variables. The differential system is solved by means of a Galerkin approach, where the unknown functions are approximated by the expressions:

$$\hat{x}(X,t) =\approx \hat{x}_M(X) + \sum_{i=1}^{r} a_i(t)\hat{\phi}_{rx}(X), \quad \hat{y}(X,t) =\approx \hat{y}_M(X) + \sum_{i=1}^{r} b_i(t)\hat{\phi}_{ry}(X) \tag{8}$$

where $\hat{x}(X)$ is the average value of $\hat{x}(X,t)$, $\hat{\phi}_{rx}(X)$ and $\hat{\phi}_{ry}(X)$ are the POMs and a_i and b_i unknowns. In Figure 2b the eigenfunctions corresponding to the first three POVs of $\tilde{X}_m$ are shown. The first five singular values of the $\tilde{X}_m$ and $\tilde{Y}_m$ that characterize the dynamics of the chain of 20 rigid links are given in the table contained in Fig. 2c. The sum of all proper orthogonal values: $\sum_j \sigma_{xj} = 12.723$ and $\sum_j \sigma_{yj} = 47.029$, respectively, with $(j = 20)$, shows that only first three POVs are enough to capture more than 99% of the "energy" contained in the data. This basis is applied to the

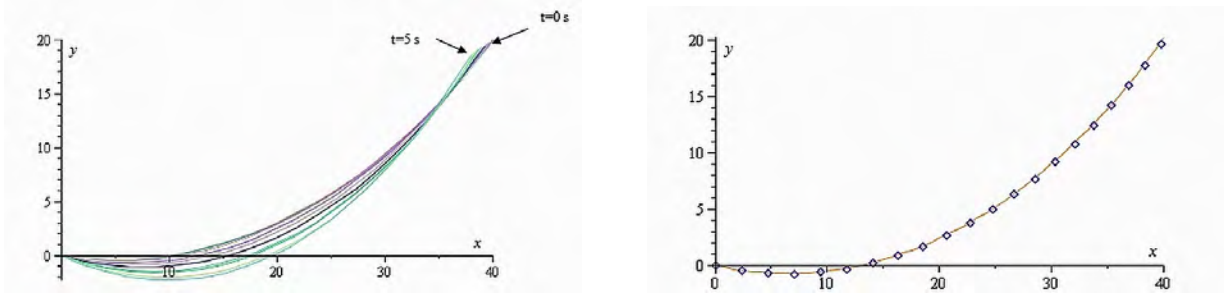

(a) (b)

Figure 3: Elastic cable dynamics example. a) Trajectory described by an elastic cable. Total time five seconds, $\omega_q = \omega_h = 0.25$rad/s. Galerkin approximation using only one POM. b)Solution for the elastic cable using four functions of the basis superimposed with the geometric static configuration at the instant $t = 2$ seconds.

dynamics of the extensible cables. In Figure 3a the resulting trajectory described by the cable during the first 5 seconds is shown, which was obtained using only one approximating function, *i.e.*, the following expression was adopted for the unknown functions:

$$\hat{x}(X,t) =\approx \hat{x}_M(X) + a_1(t)\hat{\phi}_{1x}(X) \quad \hat{y}(X,t) =\approx \hat{y}_M(X) + b_1(t)\hat{\phi}_{r1}(X) \tag{9}$$

It can be seen that, for the prescribed motion at the right end,*i.e.*, slow motion and low frequency, the cable keeps its catenary shape. This fact can be seen more clearly in Figure 3b. The solution for the extensible cable using four functions of the basis is superimposed to the geometric static configuration at the instant $t = 2$ seconds. Both are equal and coincident with a catenary curve with the same ending points. Next, other case in which a higher frequency motion is imposed at the right end, is shown. Data are the same as previous although in this case $\omega_q = 1.5$ rad/s and $\omega_h = 0.75$ rad/s. In Figure 4 the geometric configuration of the cable is shown at $t = 2$ seconds, taking one, two, three and four approximating functions to find the solution together with the geometric configuration that adopts at that same instant a chain with 40 rigid links.

5. THREE-DIMENSIONAL CABLE

Next, a three-dimensional model of a slack cable that takes into account bending and torsional stiffness is stated. The partial differential equations are then discretized using finite elements and a ROM is found using basis derived from a POD appplied to a very accurate solution from a simulation.

6. Model statement and equations of motion

In order to create a numerical model that includes the desired bending and torsional effects, it is necessary to derive the dynamic equations for a continuous cable considering the tortuous space curve, or profile, that the strained cable centerline attains in three-dimensional space. In general, the cable is modelled as a slender flexible rod under environmental, gravitational and buoyancy forces. Of particular relevance to this work was Nordgren's presentations (Nordgren, 1974) of the vector equations of motion for a continuos cable (Figure 5) which are

$$\mathbf{F}' + \mathbf{q} = \left(\frac{1}{4}\pi d^2 \rho_c \mathbf{I}\right)\ddot{\mathbf{r}}; \quad \mathbf{M}' + \mathbf{r}' \times \mathbf{F} + \mathbf{m} = \mathbf{0} \tag{10}$$

ISSN 2176-5480

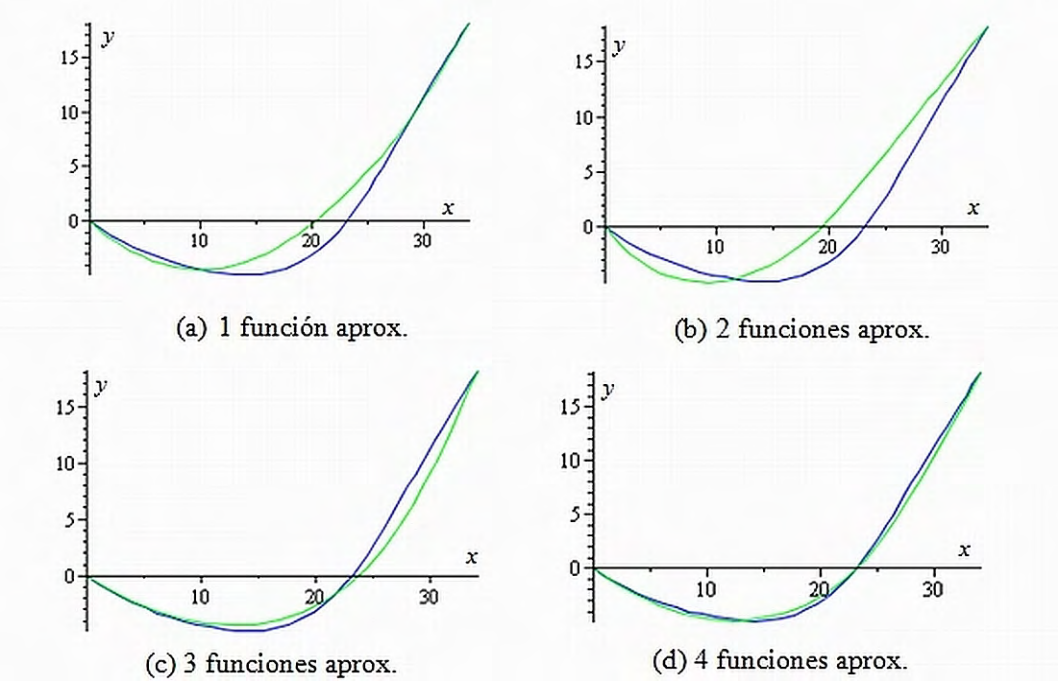

Figure 4: Geometric configuration of the cable at $t = 2$ seconds, taking (a)one, (b)two, (c)three and (c) four approximating functions, together with the geometric configuration that adopts at that same instant a chain with 40 rigid links.

where ρ_c is the density of the cable, d is the diameter of the cable, $\mathbf{r}(s,t)$ is a position vector describing the space curve formed by the center line of the cable, $\mathbf{q}$ is the vector of applied forces per unit length, $\mathbf{m}$ represents the applied moment per unit length, $\mathbf{F}$ is the vector of internal forces, $\mathbf{M}$ is the vector of internal moments, $\mathbf{I}$ is a 3×3 identity matrix, $(')$ denotes differentiation with respecto to s, the unstretched curvilinear coordinate along the cable, and $(\dot{})$ denotes differentiation with respect to time t. We express $\mathbf{r}(s,t)$ in terms of an inertial frame of reference (X, Y, Z), where X and Y point in perpendicular horizontal directions, and Z is aligned with the gravity direction. The rotational inertia of the cable is considered to be much smaller than the other terms of Eq. (10) and is thus neglected (Burgess, 1993). The dynamic equations are formulated using two local frames of reference, the Frenet frame and a frame of reference oriented with the principal axes of the cable, see Figure 5.

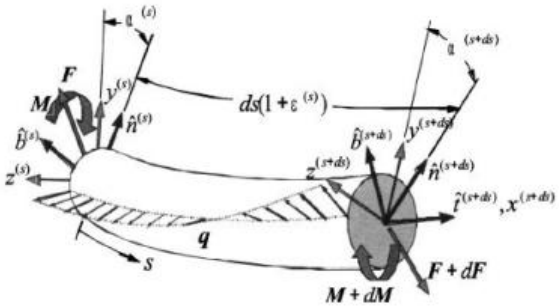

Figure 5: View of a differential segment of the cable Buckham *et al.* (2003).

The Frenet frame $(\hat{\mathbf{t}}, \hat{\mathbf{n}}, \hat{\mathbf{b}})$ is oriented with the space curve formed by $\mathbf{r}(s,t)$. As the curve $\mathbf{r}(s,t)$ is traced, the changing orientation of the Frenet frame is quantified by two parameters: the curvature κ, and the torsion γ. Assuming the strain $\epsilon \ll 1$, the basis unit vectors are defined as :$\hat{\mathbf{t}} = \mathbf{r}'$, $\hat{\mathbf{n}} = \mathbf{r}''/\kappa$, and $\hat{\mathbf{b}} = (\mathbf{r}' \times \mathbf{r}'')\kappa$ and their gradients are defined as $\hat{\mathbf{t}}' = \kappa\hat{\mathbf{n}}$, $\hat{\mathbf{n}}' = -\gamma\hat{\mathbf{b}} - \kappa\hat{\mathbf{t}}$, and $\hat{\mathbf{b}}' = \gamma\hat{\mathbf{n}}$. The curvature, κ, denotes the bend of the cable within an osculating plane that is formed by $\hat{\mathbf{t}}$ and $\hat{\mathbf{n}}$ at the considered point. Both κ and γ are defined in terms of the spatial derivatives of the space curve $\kappa = (\mathbf{r}'' \cdot \mathbf{r}'')^{1/2}$ and $\gamma = \frac{\mathbf{r}' \cdot (\mathbf{r}'' \times \mathbf{r}''')}{\kappa^2}$. The torsion of the curve γ is the spatial rate of change of the osculating plane orientation about the tangent vector, and consequently the orientation of the bend, about the tangent vector, $\hat{\mathbf{t}}$. As such, the torsion represents the twist experienced within the cable due to the shape of the cable profile. However, when the twist of the cable is considered, one recognizes that torsional couples applied at the boundaries of a cable section create an additional angular displacement, α (the torsion deformation). Thus, we introduce the body fixed reference frame (x, y, z)

ISSN 2176-5480

which remains aligned with the principal axes of the cross section, as shown in Fig.5, and is separated from the Frenet frame by an angle α about the tangent direction. As discussed by Love, the internal moment, $\mathbf{M}$, generated at any point within the cable is proportional to the curvature and the twist observed at the point (Love, 1944) $\mathbf{M} = EI\kappa\hat{\mathbf{b}} + GJ\tau\hat{\mathbf{t}}$ where E and G are the elastic and shear modulus, I is the area moment of inertia and J is the polar moment of inertia. The overall twist τ, of the cable at the point is given by $\tau = \gamma + \alpha'$ Following Garret (1982) and Nordgren (1974), and assuming that there are no external moments applied between the cable boundaries ($\mathbf{m} = \mathbf{0}$), a definition for the vector of internal forces at any location along the cable can be written

$$\mathbf{F} = T\hat{\mathbf{t}} - EI\kappa'\hat{\mathbf{n}} - EI\kappa\gamma\hat{\mathbf{b}} + GJ\tau\kappa\hat{\mathbf{b}}. \tag{11}$$

where T is defined below, and the spatial derivative κ' is a nonlinear function of the spatial coordinate s, which complicates the finite element procedure that will be used. After some algebra it is possible to eliminate κ' in Eq. (11), obtaining the following

$$\mathbf{F} = -(EI\kappa\hat{\mathbf{n}})' + (T - EI\kappa^2)\hat{\mathbf{t}} + GJ\tau\kappa\hat{\mathbf{b}} \tag{12}$$

where the term $-EI\kappa^2$ is included to cancel the spurious component of the internal force induced when considering the tangential component due to changing of $\hat{\mathbf{n}}$. The internal force, T, is defined using the constitutive relationship (a visco-elastic material) $T = EA\epsilon + C_{ID}\dot{\epsilon}, \qquad \epsilon = [(\mathbf{r}' \cdot \mathbf{r}')^{1/2} - 1]$ where ϵ is the strain and C_{ID} is an internal viscous damping coefficient. This simple viscous damping model is used to represent the dissipation of energy within the cable via friction between the layers of conductors, armor, and polymer coatings of a typical cable. Equation (12) defines the internal force as an explicit function of the cable's elastic deformation as defined by the axial strain, curvature, and twist. Substituiting Eq. (12) into Eq. (10) reduces the two original vector equations of motion to a single vector equation that defines the translational motion in terms of these three elastic deformations, and a scalar constraint equation that defines the variation of the twist along the cable:

$$-(EI\mathbf{r}'')'' + [(T - EI\kappa^2)\mathbf{r}']' + [GJ\tau(\mathbf{r}' \times \mathbf{r}'')]' + \mathbf{q} = \left(\frac{1}{4}\pi d^2\rho_c\mathbf{I}\right)\ddot{\mathbf{r}}; \qquad (GJ\tau)' = 0. \tag{13}$$

In this work, the applied force vector $\mathbf{q}$ consists of the distributed weight and buoyancy.

6.1 Finite Elements discretization

In the discretization process it is necessary to find a suitable approximations to both $\mathbf{r}(s,t)$ and $\alpha(s,t)$. Applying a finite element approach, the cable is considered as a contiguous set of N cubic segments, or elements, which have the same physical properties as the continuous cable. The trial solution $\mathbf{r}_i$ and α_i, defines the state of the i^{th} cable element extending between the nodes $i-1$ and i of the discrete cable. The shape of the element, $\mathbf{r}_i$, is defined in terms of the position and curvature vectors observed at the $i-1$ and i^{th} node points:

$$\mathbf{r}(s,t) : s \in [s^{(i-1)}, s^{(i)}] \approx \mathbf{r}_i, \qquad \mathbf{r}_i = \mathbf{r}^{(i-1)}\phi_{i,1}(s) + \mathbf{r}''^{(i-1)}\phi_{i,2}(s) + \mathbf{r}^{(i)}\phi_{i,3}(s) + \mathbf{r}''^{(i)}\phi_{i,4}(s) \tag{14}$$

As is discussed in detail in (Buckham *et al.*, 2004), the element is a twisted cubic spline. The element shows a $\mathcal{C}^2(s)$, or second order, continuity across the node points to reflect the continuity expected in the curvature. The element is a superposition of a linear combination of the node points and a cubic refinement that interpolates the node curvature vectors.The shape functions are given by:

$$\phi_{i,1} = \frac{s_i - s}{L_e}, \qquad \phi_{i,2} = \frac{1}{6}\left(\phi_{i,1}^3 - \phi_{i,1}\right)L_e^2 \qquad \phi_{i,3} = \frac{s - s_{i-1}}{L_e}, \qquad \phi_{i,4} = \frac{1}{6}\left(\phi_{i,3}^3 - \phi_{i,3}\right)L_e^2 \tag{15}$$

where L_e is the length of the discrete cable elements. The specification of the $\mathcal{C}^2(s)$ continuity produces a system of tridiagonal linear equations that allow the curvature to be calculated from the node positions at any instant in the simulation. The element type thus minimizes the state variables required to define the cable shape at any time - the six position variables of the element node points. The trial solution is completed by modelling the torsional deformation within the element, α_i, as a linearly varying quantity between the node points $\alpha_i = \alpha_{i-1}\phi_{i,1}(s) + \alpha_i\phi_{i,3}(s)$. The optimum coefficients of the two polynomials are obtained through the application of Galerkin's criterion over the domain of the general element i^{th} element. The evaluation of the Galerkin residuals is described in (Buckham *et al.*, 2004), including the various representations for the variation of the enviromental and internal effects over the element. The results of this procedure are the element equations given by:

$$([\mathbf{K}_B]_i + [\mathbf{K}_A]_i + [\mathbf{K}_\tau]_i)\,\mathbf{X}_i + \mathbf{W}_i + \mathbf{H}_i + \mathbf{B}_i = [\mathbf{M_e}]_i\ddot{\mathbf{X}}_i \tag{16}$$

and,

$$\frac{GJ}{L_e}\begin{bmatrix} 1 & -1 \\ -1 & 1 \end{bmatrix}\begin{Bmatrix} \alpha_{i-1} \\ \alpha_i \end{Bmatrix} = GJ\begin{Bmatrix} \gamma_{i-1/2} \\ -\gamma_{i-1/2} \end{Bmatrix} + \begin{Bmatrix} -GJ\tau_i^{i-1} \\ GJ\tau_i^i \end{Bmatrix} \tag{17}$$

ISSN 2176-5480

where the boundary terms $GJ\tau_i^{i-1}$ and $GJ\tau_i^i$ represent the internal restoring torque at the boundaries of the element.

The 12×12 system matrices $[\mathbf{K}_B]_i$, $[\mathbf{K}_A]_i$ and $[\mathbf{K}_\tau]_i$ embody generalized bending, axial and torsional forces, respectively, that are applied at the element nodes and result from the curvature, axial strain and twist experienced throughout the cable element. The generalized load vectors $\mathbf{W}_i$, $\mathbf{H}_i$ and $\mathbf{B}_i$ define de gravitational, hydrodynamic, and applied forces respectively, and the 12×1 vector, $\mathbf{X}_i = \left\{ \mathbf{r}_{i-1}^T, \mathbf{r}_{i-1}'^T, \mathbf{r}_i^T, \mathbf{r}_i'^T \right\}^T$, defines the element trial solution.

The symmetric element mass matrix, $[\mathbf{M}_e]_i$ is reduced to a lumped mass matrix. This reduction effectively redistributes the cable mass such that it is concentrated at the node locations. A consequence of this reduction is the elimination of the time derivatives of the curvature vectors from the right hand side of Eq.(16) which reflects the fact that changes in the cubic element shape of the element, caused by changing curvature at the element end nodes, do not accelerate any cable mass. Through the lumped mass approximation, Eq.(16) is reduced to a system of 6 equations (rather than 12) by premultiplying both sides by

$$\mathbf{P} = \begin{bmatrix} \mathbf{1} & \frac{1}{L_e}\mathbf{1} & \mathbf{0} & \mathbf{0} \\ \mathbf{0} & \mathbf{0} & \mathbf{1} & \frac{1}{L_e}\mathbf{1} \end{bmatrix} \tag{18}$$

where $\mathbf{1}$ is a 3×3 identity matrix. The pre-multiplication by $\mathbf{P}$ transforms the 12×12 system matrices and 12×1 load vectors into 6×12 system matrices and 6×1 quantities, respectively, that given the temporal change of the element's 6 state variables, the node positions. It is these reduced matrices and vectors that are the basis for the model assembly.

Applying the element Eqs. (16) and (17) for each node in the concatenation of elements, $0 \leq i \leq N$, a global system of equations of motion and twist constraints are produced. The form of the assembled equations is

$$\ddot{\mathbf{R}} = \mathbf{F}(t, \mathbf{R}, \dot{\mathbf{R}}); \qquad \text{where } \mathbf{R} = \left\{ \mathbf{r}^{(0)T}, \mathbf{r}^{(1)T}, \ldots, \mathbf{r}^{(N)T} \right\}^T \tag{19}$$

Equation (19) is a series of $3(N+1)$ second order differential equations. Given a set of initial conditions $\mathbf{R_0} = \mathbf{R}(t = 0)$ and $\dot{\mathbf{R}}_\mathbf{0} = \dot{\mathbf{R}}(t = 0)$ the model can evolve in time by the specification of boundary conditions and the provision of a suitable integration routine.

7. MODEL ORDER REDUCTION

The main idea of model reduction is to find a spatial repesentation of the primary variable $\mathbf{R}$, which would ensure the response of the full and reduced models to be close in certain sense, and which would be at the same time much faster than the full FE model. In other words, we would like to find a representation minimizing the number of degrees of freedom needed in the computation to reach a certain error level (measured with respect to the full FE model). Most reduction methods for nonlinear dynamic finite element analysis are based on projection onto a finite dimension subspace. The original motion given by the position vector $\mathbf{R}$ is projected onto a subspace where the projection is described by

$$\mathbf{R}(t) = \mathbf{Q}\,\mathbf{q}(t) \tag{20}$$

where $\mathbf{q}(t) \in \mathbb{R}^k \subset \mathbb{R}^n$ is the motion in the subspace. The columns of the transformation matrix $\mathbf{Q} \in \mathbb{R}^{n \times k}$ are the basis vectors, which span the subspace. Inserting Eq. (20) into the dynamic equilibrium (Eq. 19) and pre-multiplying by $\mathbf{Q}^T$ (that is, projecting in the subspace spanned by) yields the reduced system

$$\mathbf{Q}^T\mathbf{Q}\ddot{\mathbf{q}}(t) = \mathbf{Q}^T\mathbf{F}(t, \mathbf{Q}\,\mathbf{q}(t), \mathbf{Q}\,\dot{\mathbf{q}}(t)) \tag{21}$$

The choice of the reduced basis clearly affects the quality of approximation. The techniques for constructing the reduced basis use a common observation that, for a particular system, the solution space is often attracted to a low-dimensional manifold. Among the various techniques for obtaining a reduced basis, Proper Orthogonal Decomposition constructs a set of global basis functions from a singular value decomposition (SVD) of *snapshots*, which are discrete samples of trajectories associated with a particular set of boundary conditions and inputs. This basis is *optimal* in the sense that a certain approximation error concerning the snapshots is minimized. Thus, the space spanned by the basis from POD often gives an excellent low-dimensional approximation. Once the reduced model has been constructed from this reduced basis, it may be used to obtain approximate solutions for a variety of initial conditions and parameter settings, provided the set of samples is rich enough. This empirically derived basis is clearly dependent on the sampling procedure.

8. NUMERICAL ILLUSTRATION

The dynamical response of a cable was analyzed by means of the above proposed finite element approach. The total length of the cable is $L = 47$m. The cable was supposed fixed at the left end with its right end subjected to prescribed motions with the following cosine functions: $X(L,t) = A_1 + a_1\cos(\omega_1 t)$, $Y(L,t) = A_2 + a_2\cos(\omega_2 t)$, $Z(L,t) = A_3 + a_3\cos(\omega_3 t)$. The following mechanical and geometrical properties were adopted: $\rho_c = 7850$ kg/m^3

ISSN 2176-5480

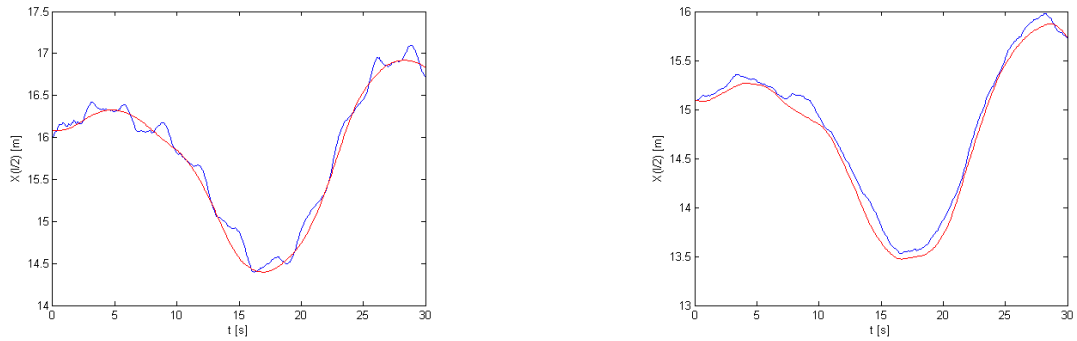

(a) (b)

Figure 6: Comparison of the finite element three-dimensional cable with elastic chain. Temporal variation of X component at the center of the cable. a) 4 element; b) 32 elements.

(density), $E = 2.1 \times 10^{11}$ N/m^2 (Young Modulus), $d = 2.85 \times 10^{-2}$ m (diameter), $C_D = 0$ (internal viscous damping). In all cases, the (unstretched) condition at initial instant was adopted to be the static solution of an inextensible cable subjected to selfweight (catenary solution) with ends coordinates $(0, 0, 0)$ and $(40, 40, 20)$. In order to check the model, a comprarison of this model with the 3D elastic chain is depicted in Figure 6. Also, the difference between the two solutions is denoted by d which is defined as $d = \|X_{chain} - X_{cable}\|/3/Nel/nt$ where Nel is the number of elements and nt the number of instants. Nel times nt is the matrix dimension and the number 3 is due to the three degrees of freedom x, y, z. Values of d are reported in the same figure.

Nel	d
4	$23.86e{-}4$
8	$9.37e{-}4$
16	$6.63e.4$
32	$4.85e{-}4$

Table 1: Comparison shown in Fig. 6. Error d

.

8.0.1 Three-dimensional cable: Example 1

In order to check the performance of the finite element model, a series of simulations with different number of elements were run. The parameters that define the prescribed motions at the end of the cable at every instant of time were adopted

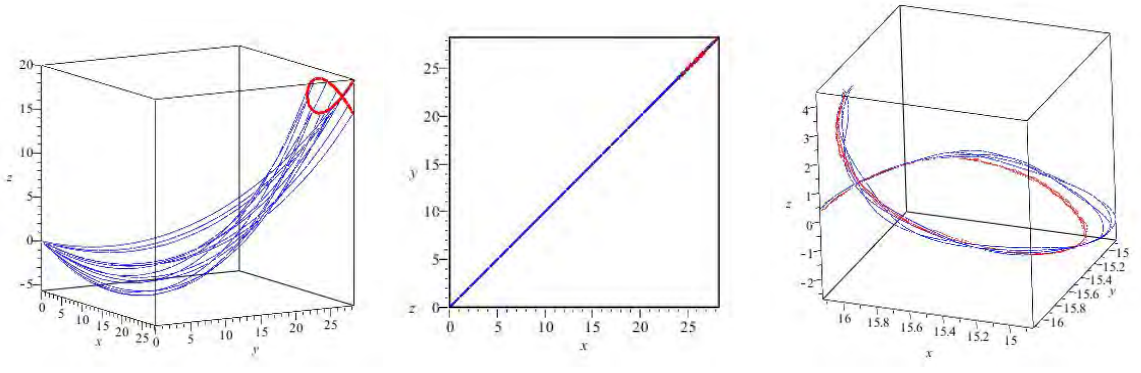

(a) (b) (c)

Figure 7: Three-dimensions cable. Example 1. a) snapshots of the cable motion at first 30 seconds and trajectory described by the end of the cable (red). FEM with 32 elements; b) xy projection of snapshots; c) Trajectory described for the midle point form both models: present FEM formulation (blue) , concentrated mass and springs formulation (red). Total time 50s, 32 elements.

as: $A_1 = A_2 = 26.16m$, $A_3 = 18$m, $a_1 = a_2 = 2.12$m, $a_3 = 2$m, $\omega_1 = \omega_2 = 0.5$ rad/s, $\omega_3 = 0.75$ rad/s. Figure (7b) depicts the motion of the chain by superposing different positions, for a total time of 10 seconds, and also their projections

ISSN 2176-5480

onto the xy plane where it can be observed that the cable stays in the same vertical plane at every instant, as expected for an initial configuration and a load contained in the same plane.

Since in this example the cable is subjected to a relative low-speed motion, a comparison with a chain under the same action is now depicted. An algorithm that deals with the dynamic of chains modelled as concentrated point mass joined by springs, is reported in (Wilson *et al.*, 2003). A 32 link chain was solved using this algorithm for a qualitative comparison with results from the present cable FEM formulation. Figure 7c shows the trajectory described by the middle point for both models. The point describes the trajectory more than once during the considered time which is reflected with various blue lines. In the two cases the same qualitative response was obtained.

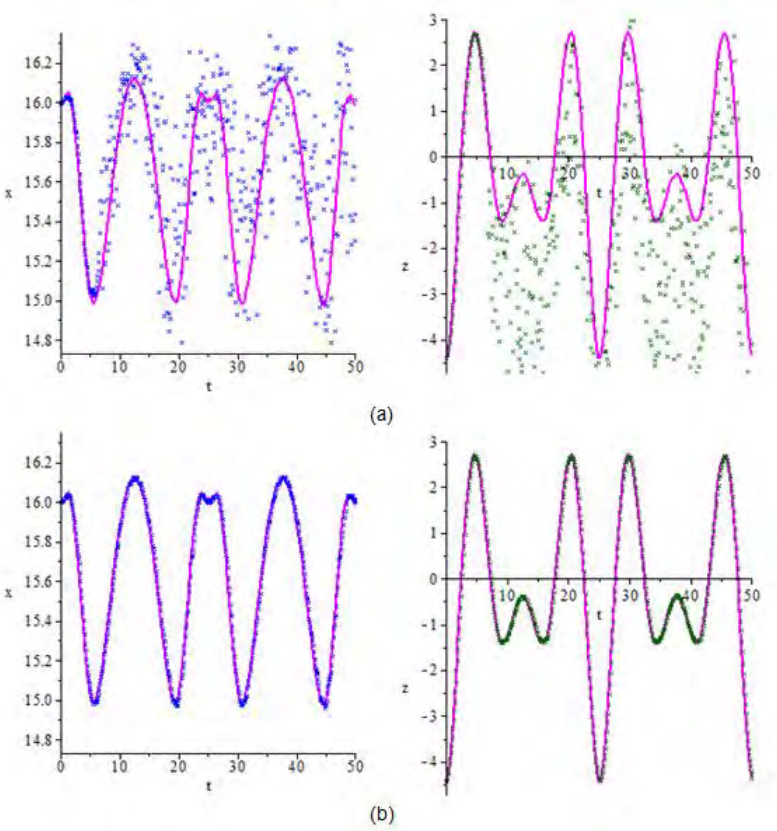

Figure 8: Example 1. Temporal variation of the center point of the cable. Left graphs: coordinate x vs. time. Right graphs: coordinate z vs. time. Fuchsia curve: FEM solution with 32 elements. Blue points: reduced order model solution with POD. a) 5 POMs, b) 6 POMs.

Now and in order to construct a reduced order model using POD, a FE simulation with 32 elements was run for a total time of 100 seconds from which the snapshots matrix was obtained (one snapshot every 0.1 seconds). Then, following the procedure detailed in Section 2the POD basis was obtained to get the $\mathbf{Q}$ projection orthogonal matrix used to reduce the dimension (degrees of freedom) of the problem .The results obtained with the reduced FE using 5 and 6 eigenvectors (Proper Orthogonal Values, POMs) corresponding to the highest 5 or 6 eigenvalues (Proper Orthogonal Values, POVs), respectively, are depicted in Figure 8. It can be observed that adding the sixth POM achieves an adequate approximation. It should be noted that the total time needed for a simulation with a reduced order model was significantly decreased compared with the full FE model. Some comments on the time reduction are included in the next example.

8.1 Example 2

The dynamics of the same cable is now analyzed but under a different motion and an angular displacement $\alpha(L,t)$ (torsional deformation) at the top right end. The following values were adopted: $A_1 = A_2 = 26.16m$, $A_3 = 18$m, $a_1 = a_2 = 2.12$m, $a_3 = 2$m, $\omega_1 = 0.5$rad/s, $\omega_2 = 0.75$rad/s, $\omega_3 = 0$rad/s, $\alpha(L,t) = \pi(1 - \cos(0.15t))$.

The first 30 seconds snapshots are depicted in Figure 9a found with the FEM with 32 elements (left graph, blue line). The right plot shows the xy projections of the snapshots, from which the out-of-plane motion is apparent. Also, the prescribed motion at the right end is plotted in red line. It should be noted that the computational time for a 6 POMS reduced model takes the 30% of the time necessary to run the non-reduced model. This feature is desirable when, for instance, one performes quantification of uncertainties that require of a large number of realizations to achieve the

ISSN 2176-5480

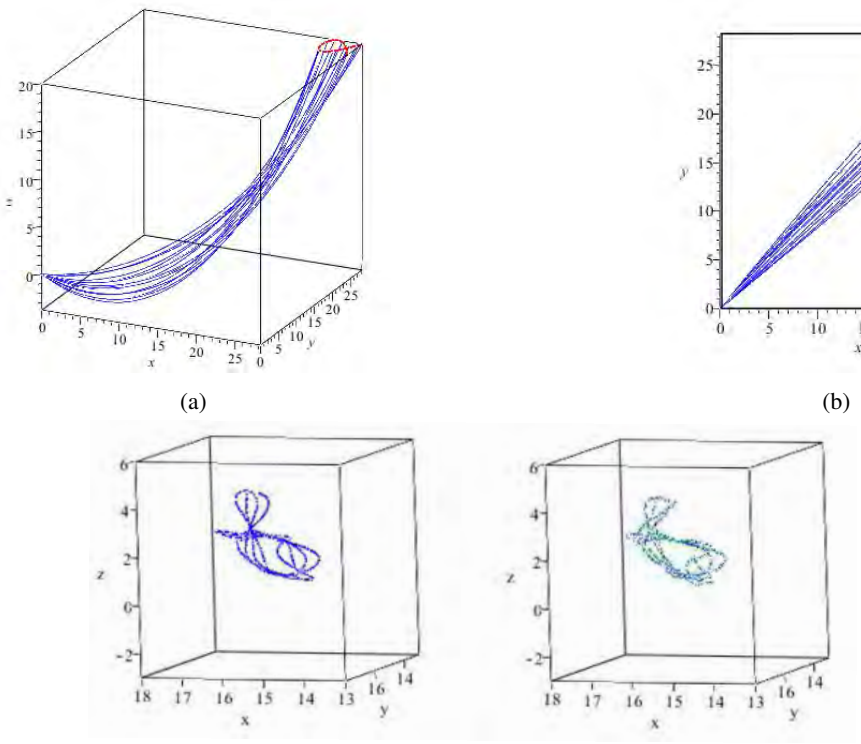

Figure 9: Example 2. a) First 30 s snapshots found with the FEM with 32 elements (blue line); b) xy projection of the snapshots (blue line). Prescribed displacement at right end (red line); c) and d) Central point trajectory. c) Left: FEM model. Simulation time of 50 s, 32 elements. Right: FEM (blue line) and reduced model with 9 POMs (green line).

statistical study.

The effect of the addition of POMs is clearly observed at Figure 10. The time history of the central point x coordinate was found for 6, 7, 8 and 9 eigenvectors (POMs). The number of POMs to approximate adequately the dynamics of the cable, appears to be 8 or 9. Finally, Figure 9c depicts the 3D trajectories found with the FEM (50 seconds, 32 elements) (left plot) and the same trajectory superimposed to the reduced order model one (9 POMs) at the right plot. Again, it is seen that the dynamics is appropriately approximated with a more efficient approach.

9. FINAL COMENTS

The dynamics of two models of slack cables was analyzed in order to obtain reduced order models (ROM) through a Proper Orthogonal Decomposition (POD). The first model deals with a 2D representation and the basis is found from a plane chain dynamics. Then a Galerkin proyection allows to construct the ROM. The second model consists in a 3D cable with bending and torsion al stiffness. The bases were derived from a very accurate finite elements model. It should be noted that in the presence of a general nonlinearity, the standard POD-Galerkin technique reduces dimensions in the sense that far fewer variables are present, but the complexity of evaluating the nonlinear term remains that of the original problem.

The dynamics of the chain and the cable are compared but they should be regarded only from the qualitative point of view. In effect, the responses at every instant are very similar but they are two different models and then, despite taking a larger number of elements either for the chain or for the cable, one does not expect a numerical convergence. Regarding the reduced order models (ROMs), the convergence study would consist on the following. The error in the dynamics of the cable modeled through a ROM using orthogonal projections on subspaces of smaller dimension, can be measured by means of the distance $d(X, X_r)$, being X and X_r the responses of the reference non-reduced model and the reduced model, respectively. However, as a certain number of POMs is considered, numerical errors arise and propagate, affecting the results. This situation is under study at present. The algorithm will be modified to reduce this unwanted effect and the conclusions will be shown at the conference.

ISSN 2176-5480

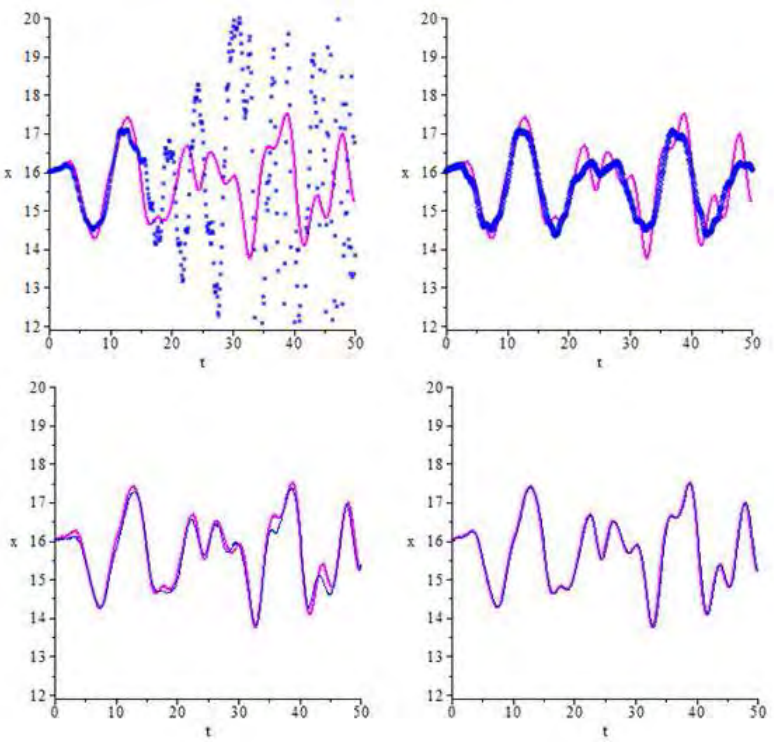

Figure 10: Example 2. Time history of the x coordinate of the midle point: 6,7,8 y 9 eigenvectors.

10. ACKNOWLEDGEMENTS

The authors are grateful to the financial support from CAPES, CNPq, and FAPERJ from Brasil, and FRCU-UTN, FRCon-UTN, SGCyT-UNS and CONICET from Argentina.

11. REFERENCES

Buckham, B., Driscoll, F. and Nahon, M., 2004. "Development of a finite element cable model for use in low-tension dynamics simulation". *ASME Jounal of Applied Mechanics*, Vol. 71, pp. 476–485.

Buckham, B. and Nahon, M., 2001. "Formulation and validation of a lumped mass model for low-tension rov tethers". *International Journal of Offshore and Polar Engineering*, Vol. 11, No. 4, pp. 282–289.

Buckham, B., Nahon, M., Seto, M., Zhao, X. and Lambert, C., 2003. "Dynamics simulation of a towed underwater system: Part i model development". *Ocean Engineering*, Vol. 30, No. 4, pp. 453–470.

Burgess, J., 1993. "Bending stiffness in a simulation of undersea cable deployment". *International Journal of Offshore and Polar Engineering*, Vol. 3, pp. 197–204.

Chaturantabut, S. and Sorensen, D., 2010. "Nonlinear model reduction via discrete empirical interpolation". *Journal of Scientific Computing*, Vol. 32, No. 5, pp. 2737–2764.

Driscoll, F., Lueck, R. and Nahon, M., 2000. "Development and validation of a lumped-mass dynamics model of a deep-sea rov system". *Applied Ocean Recearch*, Vol. 22, No. 3, pp. 169–182.

Escalante, M., Filipich, C. and Rosales, M., ???? "Karhunen-Loeve Decomposition and Model Order Reduction applied to the Non-linear Dynamics of an Extensible Cable".

Esmailzadeh, E. and Goodarzi, A., 2001. "Stability analysis of a CALM floating offshore structure". *International Journal of Non-Linear Mechanics*, Vol. 36, No. 6, pp. 917–926.

Filipich, C. and Rosales, M., 2000. "A further study on the postbuckling of extensible elastic rods". *International Journal of Non-Linear Mechanics*, Vol. 35, No. 6, pp. 997–1022.

Filipich, C. and Rosales, M., 2007. "Dynamic Analysis of plane mooring chains of inextensible links". In *Mecánica Computacional*. Vol. 26, pp. 2479–2495.

Garret, D., 1982. "Dynamic analysis of slender rods". *ASME Journal of Energy Resources Technology*, Vol. 104, pp. 302–306.

Grosenbaugh, M., Howell, C. and Moxnes, S., 1993. "Simulating the dynamics of underwater vehicles with low tension tethers". *International Journal of Offshore and Polar Engineering*, Vol. 3, No. 3, pp. 213–218.

Hoetelling, H., 1935. "Simplified calculation of principal component analysis". *Psychometrica*, Vol. 1, pp. 27–35.

Huang, S., 1994. "Dynamic analysis of three-dimensional marine cables". *Ocean Engineering*, Vol. 21, No. 6, pp.

ISSN 2176-5480

587–605.

Karhunen, K., 1946. "Zur spektraltheorie prozesse". *Annales Academiae Scientiarum Fennicae, Ser. A*, Vol. 34.

Kunisch, K. and Volkwein, S., 2008. "Proper orthogonal decomposition for optimality systems". *Mathematical Modelling and Numerical Analysis*, Vol. 42, No. 1, pp. 1–23.

Liu, Y. and Bergdahl, L., 1997. "Frequency-domain dynamic analysis of cables". *Engineering Structures*, Vol. 19, No. 6, pp. 499–506.

Loève, M., 1946. "Fonctions aleatoire de second ordre". *Revue*, Vol. 48, pp. 195–206.

Love, A., 1944. *A Treatise on the Mathematical Theory of Elasticity*. Dove, New York, 4th edition.

Nordgren, R., 1974. "On the computation of the motion of elastic rods". *ASME Jounal of Applied Mechanics*, Vol. 41, pp. 777–780.

Nordgren, R., 1982. "Dynamic analysis of marine risers with vortex excitation". *ASME Journal of Applied Mechanics*, Vol. 104, pp. 14–19.

Pascoal, R., Huang, S., Barltrop, N. and Guedes Soares, C., 2005. "Equivalent force model for the effect of mooring systems on the horizontal motions". *Applied Ocean Research*, Vol. 27, No. 3, pp. 165–172.

Rosales, M. and Filipich, C., 2006. "Full modeling of the mooring non-linearity in a two-dimensional floating structure". *Int. Journal of Nonlinear Mechanics*, Vol. 41, pp. 1–17.

Simo, J., 1985. "A finite strain beam formulation. the three-dimensional dynamic problem. part i: Formulations and optimal parametrization". *Computational Methods in Applied Mechanics and Engineering*, Vol. 49, pp. 55–70.

Sirovich, L., 1987. "Turbulence and the dynamics of coherent structures. i-iii". *Quarterly of applied mathematics*, Vol. 45, No. 3, pp. 561–590.

Walton, T. and Polacheck, H., 1960. "Calculation of transient motion of submerged cables". *Mathematics of Computation*, Vol. 14, No. 69, pp. 27–46.

Wilson, H., Turcotte, L. and Halpern, D., 2003. *Advanced mathematics and mechanics applications using MATLAB*. CRC press.

12. RESPONSIBILITY NOTICE

The authors are the only responsible for the printed material included in this paper.